Title

Tracking the Local Effect of Fluorine Self-Doping in Anodic TiO2 Nanotubes

Journal

The Journal of Physical Chemistry C, 120(8)

ISSN

1932-7447

Authors

Li, Jun

Liu, Changhai

Ye, Yifan

et al.

Publication Date

2016-03-03

DOI

10.1021/acs.jpcc.5b11445

Peer reviewed

THE JOURNAL OF PHYSICAL CHEMISTRY C

Article

pubs.acs.org/JPCC

Tracking the Local Effect of Fluorine Self-Doping in Anodic TiO_2 Nanotubes

Jun Li,[†] Changhai Liu,[‡] Yifan Ye,[§,∥] Junfa Zhu,[§] Suidong Wang,[‡] Jinghua Guo,[∥,⊥] and Tsun-Kong Sham*[,†,‡]

[†]Department of Chemistry, University of Western Ontario, 1151 Richmond Street, London, Ontario N6A5B7, Canada

[‡]Soochow University−Western University Joint Centre for Synchrotron Radiation Research, Institute of Functional Nano & Soft Materials (FUNSOM), Soochow University, Suzhou, Jiangsu 215123, People's Republic of China

[§]National Synchrotron Radiation Laboratory and Collaborative Innovation Center of Suzhou Nano Science and Technology, University of Science and Technology of China, Hefei, Anhui 230029, People's Republic of China

[∥]Advanced Light Source, Lawrence Berkeley National Laboratory, Berkeley, California 94720, United States

[⊥]Department of Chemistry and Biochemistry, University of California, Santa Cruz, California 95064, United States

Supporting Information

ABSTRACT: We report herein a study in which we reveal the role of F^- incorporated in the very anodic TiO_2 nanotubes prepared electrochemically from a Ti foil using a fluoride based electrolyte. X-ray absorption near edge structure (XANES), resonant X-ray emission spectroscopy (RXES), and X-ray photoelectron spectroscopy (XPS) have been used to examine the as-prepared and the annealed TiO_2 nanotubes. It is found that the additional electron resulting from the substitution of O^{2-} by self-doped F^- in the TiO_2 lattice is localized in the t_{2g} state. Consequently, a localized Ti^{3+} state can be tracked by a d−d energy loss peak with a constant energy of 1.6 eV in the RXES, in contrast to TiO_2 nanostructures where this peak is hardly noticeable when F^- is driven out of the lattice upon annealing.

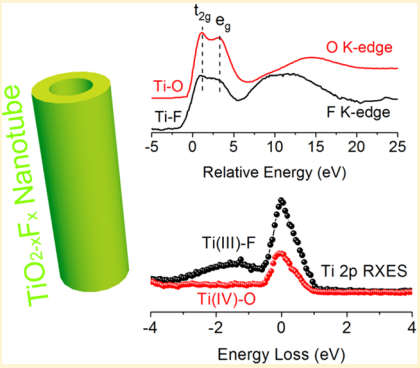

INTRODUCTION

As one of the solar-driven substrates for photovoltaics, TiO_2 and its derivatives have been extensively developed[1−3] and thoroughly investigated,[4−6] to harvest their high photocatalytic efficiency, in recent decades. Various efforts have been devoted to the morphology exploration and optimization of TiO_2 nanostructures associated with diverse applications.[2,7−9] Typically, morphology engineering of TiO_2 nanostructures using proper reactants via etching or doping is crucial to obtaining the equilibrium morphology with high surface stability and reactivity.[2,7,10] Among them, F^- deserves the most credit for the engineering of desired morphology for TiO_2 nanostructures, particularly in the preparation of high-aspect-ratio TiO_2 nanotubes (NTs). The use of proper fluoride electrolyte (e.g., HF, NH_4F) during Ti anodization can not only form and sustain the nanotubular structure, but also optimize the NT architecture with desired geometry and alignment.[11] The as-prepared TiO_2 NTs aligned vertically on the Ti substrate provide not only the unidirectional electrical channel but also a large surface area,[8,12,13] making this type of nanostructure a potential candidate for water-splitting,[8,13] solar cell,[14,15] and lithium ion battery[16,17] applications, among many others.[18−20]

However, it appears that, in F-etched TiO_2 nanostructures, a significant amount of F^- ions is self-doped (trapped) into the as-prepared samples.[11,21] Although these self-doped F^- ions can be driven out via a heating process,[7] they also have a desired effect on the functionality of the as-obtained TiO_2 nanomaterials. As a matter of fact, TiO_2 doping with fluorine has long been demonstrated both experimentally and theoretically, which results in the introduction of F 2p states and its concomitant Ti^{3+} states in the band gap of TiO_2, leading to the enhanced light absorption of TiO_2 toward the visible and thus the increase of photoactivity.[22,23] As for anodic TiO_2 NTs, the amorphous form (as-grown with a large amount of F^- ions) is reported to be a promising anode material for both lithium ion and sodium ion batteries,[16,24] in which the self-doped F^- ions and concomitant Ti^{3+} species might enhance battery performances (e.g., increase charge carrier density and facilitate electron transfer). More interestingly, by applying a sealed annealing procedure, self-doped F^- ions play a critical role in amorphous-to-anatase phase transformation, in which amorphous TiO_2 NTs will be tailored into truncated tetragonal bipyramidal

Received: November 23, 2015
Revised: February 10, 2016
Published: February 16, 2016

DOI: 10.1021/acs.jpcc.5b11445
J. Phys. Chem. C 2016, 120, 4623−4628

anatase nanocrystals (NCs), exposing their {001} facets, where the size and percentage of {001} facets of the as-obtained NCs highly depend on the concentration of the self-doped F^- ions in the amorphous NTs.[21,25] Therefore, electronic structure investigation of the local effect of self-doped F^- ions to the titania matrix holds paramount significance in the understanding of such phenomena. Two issues need to be addressed. First, the location of doping centers of F^- in the oxide matrix needs clarification, which is also under debate in the literature.[26] Second, the distribution of the extra electron introduced from F^- substitution of O^{2-} lacks concrete evidence although the formation of Ti^{3+} resulting from the fluorine doping in TiO_2 is supported by charge neutrality considerations and theoretical calculations using hybrid density functional theory (DFT) calculations.[26]

In this work, we report a comprehensive study to reveal the electronic structure and the lattice location of the self-doped F^- ions in the matrix of TiO_2 NTs using X-ray absorption near edge structure (XANES), which probes the unoccupied electronic densities of states. The local effect of F self-doping on the occupied electronic states of TiO_2 NTs is also investigated using resonant X-ray emission spectroscopy (RXES), which is also referred to as resonant inelastic X-ray scattering (RIXS).[27−29]

EXPERIMENTAL SECTION

Synthesis of Anodic TiO_2. The electrochemical anodization method was applied to grow TiO_2 NTs using a custom-made two-electrode electrochemical cell in which a Ti foil (1 cm × 2 cm with a thickness of 0.1 mm, Goodfellow) was used as the anode whereas the cathode was a Pt wire, and a dc power supply (Hewlett-Packard, 6209B) was used for the anodization process: the two electrodes with a distance of 2 cm were soaked into the electrolyte (~80 mL) consisting of 0.3 wt % NH_4F (98.0% minimum, ACS, Alfa Aesar), 2 vol % deionized water and ethylene glycol; then an electrical voltage at 50 V at room temperature was applied to the cell for 12 h to obtain the NT layer attached on the Ti substrate. The whole film was rinsed with ethanol several times to remove the excess electrolyte and dried with N_2 gas, and then cut into two pieces. The first piece was kept as is and is denoted "as-prepared NT" (APNT); the second one was annealed under 450 °C in ambient air for 2 h with a heating rate of 5 °C min^{-1} to achieve the anatase phase using a muffle furnace, denoted "NT450".

Characterization. Scanning electron microscopy (SEM) images and energy dispersive X-ray (EDX) spectroscopy were recorded using a LEO (Zeiss) 1540 XB SEM at the Nanofabrication Laboratory, University of Western Ontario (ON, Canada). The SEM is equipped with an EDX detector operating at 10 kV. X-ray photoemission spectroscopy (XPS) was conducted under ultrahigh vacuum using monochromatic Al Kα as the X-ray source (Kratos Axis Ultra DLD). The glancing angle of the incident X-ray photon beam is ~40°, and the XPS analyzer is at the magic angle (~54°) with respect to the incident beam. The binding energy of XPS spectra was calibrated to 284.6 eV using the C 1s photoelectron peak as the reference. XANES spectra were measured at the Canadian Light Source (CLS) located on the campus of the University of Saskatchewan (SK, Canada). The Ti $L_{3,2}$-edge, O K-edge, and F K-edge were recorded at the high resolution spherical grating monochromator (SGM) beamline with an energy resolution of $E/\Delta E \geq 5000$,[30] and all the edges of interest were measured from well below to above the absorption threshold of different edges. Two modes were used to collect XANES spectra: surface-sensitive total electron yield (TEY) mode using the specimen current and bulk-sensitive X-ray fluorescence yield (FLY) mode using four silicon drift detectors (SDD). Specifically, like XPS, TEY has a detection depth on the order of nanometers due to the shallow electron escape depth. FLY, on the other hand, collects out-going fluorescent X-rays and has a penetration depth on the order of 10^2 nm within the photon energy range measured in this work.[9] For XANES detection, a glancing angle of 45° between the photon beam and the surface of TiO_2 NTs (attached on the sample holder) was used, of which TEY was collected by monitoring the specimen current, whereas FLY was measured with the fluorescence detectors having an angle of ~90° to the incident beam. All XANES spectra were calibrated to the incident photon flux. The Ti 2p RXES spectra collection was carried out at beamline 8.0.1 at the Advanced Light Source (ALS), Lawrence Berkeley National Laboratory (LBNL, Berkeley, CA, USA); the glancing angle of incidence was ~30° toward the top region of TiO_2 NTs. The resolution was set to 0.4 eV with a high resolution grating spectrometer[28] at various constant excitation energies near the Ti 2p absorption threshold during Ti 2p RXES spectra collection.

RESULTS AND DISCUSSION

The SEM images of the as-prepared NTs (APNT) prepared by electrochemical etching of a Ti foil in an NH_4F solution are shown in Figure 1a,b, in which the well-ordered NTs are closely

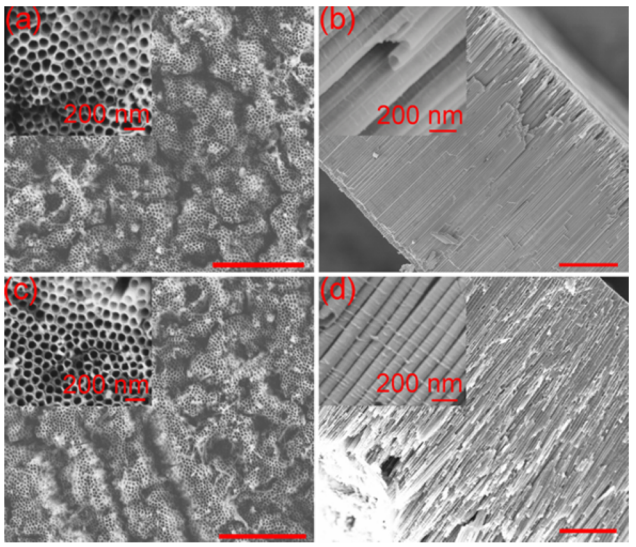

Figure 1. SEM images with top and cross-section views of APNT (a, b) and NT450 (c, d). All the scale bars in (a)−(d) are 3 μm. The magnified views are located in their top left insets.

packed with an average pore size of ~60 nm, a wall thickness of ~15 nm, and a length of ~15 μm. Energy dispersive X-ray (EDX) analysis (Figure S1 in the Supporting Information) of APNT shows its dominant Ti and O components as well as ~14.5% F (Table S1). Upon thermal annealing in ambient air at 450 °C to initiate anatase crystallization (Figure S2),[31] the NT morphology (Figure 1c,d) remains intact although most of the F^- ions are driven out with a remainder of 1.61% (Table S1) in the TiO_2 matrix.

The surface chemical states of APNT and NT450 are revealed by X-ray photoelectron spectroscopy (XPS), in which

DOI: 10.1021/acs.jpcc.5b11445
J. Phys. Chem. C 2016, 120, 4623−4628

the Ti 2p, O 1s, and F 1s as well as the valence band are tracked. As shown in Figure 2a, the Ti 2p XPS spectrum of

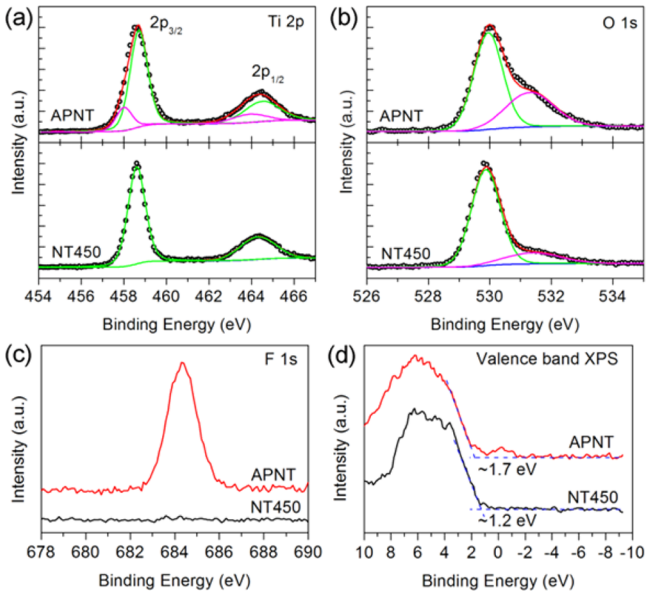

Figure 2. Normalized Ti 2p (a) and O 1s (b) XPS spectra of APNT (top) and NT450 (bottom), in which the black circles are the experimental data whereas the solid lines are fitted XPS spectra. F 1s (c) and valence band (d) XPS spectra of APNT and NT450.

NT450 displays two peaks at 458.6 and 464.3 eV, corresponding to the Ti^{4+} $2p_{3/2}$ and $2p_{1/2}$, respectively.[32] For APNT, the two Ti 2p peaks are broader and skew toward lower binding energy. Curve fitting of the XPS profile of APNT reveals shoulder features at 458.0 and 463.9 eV, which are attributed to the $2p_{3/2}$ and $2p_{1/2}$ of Ti^{3+}, respectively.[33] The O 1s XPS spectra of APNT and NT450 (Figure 2b) exhibit a dominant peak at 529.9 eV and a high energy shoulder at 531.4 eV, of which the former can be assigned to Ti−O bonding in TiO_2 whereas the latter originates from Ti−OH species on the NT surface.[32,34] The relatively intense peak of APNT at 531.4 eV suggests the abundance of hydroxyl groups attached on the F-doped amorphous NT surface. Consistent results are shown in the F 1s XPS spectra (Figure 2c): APNT displays an intense F 1s peak at 684.3 eV associated with surface fluorination of TiO_2 (formation of surface Ti−F bond),[26,34] whereas the F 1s XPS signal from NT450 becomes unnoticeable, indicating that all the F species are driven out from the NT surface after annealing at 450 °C. The formation of surface Ti−F bonds in APNT is not a total surprise considering the rich F^- environment during TiO_2 NT formation and the almost identical ionic radii between O^{2-} and F^- ions. Concomitantly, a compatible amount of Ti^{3+} surface states are formed (Figure 2a) to maintain the electroneutrality of the $TiO_{2-x}F_x$ system according to the polaron theory.[26] Therefore, the F-rich NT surfaces can attract more hydroxyl groups (Figure 2b) due to the existence of Ti^{3+} surface species and the enhanced hydrophilicity.[32] The influence of F self-doping to the valence band states of TiO_2 NT is also tracked by valence band XPS (Figure 2d). By linear extrapolation of the valence peak to the baseline, the valence band maximums of APNT and NT450 are hence determined to be ∼1.7 and ∼1.2 eV binding energy, respectively, in which the higher binding energy of the former might account for the larger band gap values of the amorphous phase than those of the anatase phase.[35] In addition, NT with F self-doping also creates an extra band state with an appreciable intensity located right above the valence band of APNT, which is also commonly observed in N-doped TiO_2 systems.[1,4,6]

However, XPS has a detection limit due to the short escape depth of low kinetic energy electrons (∼5 nm); thus XPS results do not provide accurate chemical and electronic information on the bulk. In this case, F 1s XPS results shown in Figure 2c only provide a surface fluorination peak at 684.3 eV; instead, previous F-doped TiO_2 studies also present a higher energy peak at ∼688.4 eV attributed to substitutional F species located in the subsurface of TiO_2.[23,32] The absence of this feature in our work suggests that the self-doped F^- ions are predominantly on the NT surface with a very limited amount doping into the internal TiO_2 lattice. Although similar XPS results were reported before, they are not well understood.[26,34] Thus, more evidence is needed to confirm the presence of F underneath the surface.

In order to further investigate the doping site (i.e., surface or bulk) and the chemical environment of F in the TiO_2 matrix, XANES is used to probe the local structure and bonding information on the specific element of interest (e.g., Ti, O, and F). Since XANES is a local probe, materials with both amorphous and crystalline structures can be characterized and differentiated due to the different local symmetry and neighboring atom of the absorbing atom. XANES at the F K-edge in comparison with those at the O K-edge are recorded in both total electron yield (TEY) and fluorescence yield (FLY) modes as shown in Figure 3. Of these yield techniques, FLY is

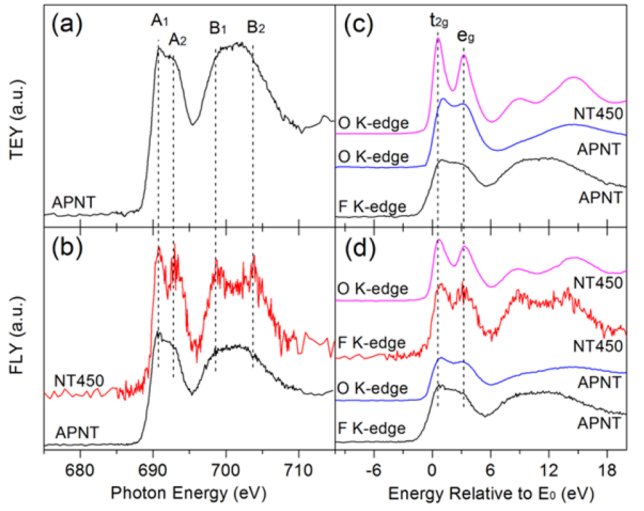

Figure 3. (a) TEY and (b) FLY XANES of APNT and NT450 recorded at the F K-edge. Alignments between O K-edge and F K-edge XANES of APNT and NT450 are recorded in (c) TEY and (d) FLY by subtracting the O K-edge and F K-edge photon energies relative to the O 1s and F 1s absorption thresholds (E_0), respectively. The lack of the TEY spectrum at the F K-edge of NT450 in both (a) and (c) is due to the release of F^- ions on the surface of NT450 after annealing.

bulk-sensitive whereas TEY is surface sensitive.[9] Two interesting features are apparent from Figure 3. First, while the F K-edge XANES of APNT is collected in both detection modes, only FLY XANES of F is present in NT450 albeit with poor statistics. This observation indicates that F^- ions are self-doped both on the surface and in the bulk of the amorphous

DOI: 10.1021/acs.jpcc.5b11445
J. Phys. Chem. C 2016, 120, 4623−4628

structure (APNT) during anodization whereas only a small amount of self-doped F^- ions is left in the bulk of the anatase phase (NT450) after annealing at 450 °C. Second, as the electronic transition from F 1s to F 2p is involved in the F K-edge XANES, four resonant peaks are shown. Both the unresolved twofold structures (D_1 and D_2; $E_1$and E_2) in APNT are well resolved after phase transformation from amorphous to anatase. The spectral pattern of the F K-edge shares a similar XANES profile with that of the O K-edge XANES when both sets of spectra are calibrated to the absorption threshold (inflection point of the rising edge). As shown in Figure 3c,d, the XANES at the F K-edge and O K-edge are well aligned, providing concrete evidence for the formation of Ti−F bonds with F^- ions being in a similar local environment as O^{2-} ions, i.e., the substitutional replacement of O^{2-} by F^- ions. The similarity comes about since O^{2-} and F^- are isoelectronic; their k dependent phases as an absorber are very similar and should yield very similar patterns if they are in the same environment. Thus, the origins of the two peaks D_1 and D_2 can be unambiguously assigned to electronic transitions from F 1s to F 2p states hybridized with Ti t_{2g} and e_g manifolds (unoccupied densities of states of F 2p−Ti 3d character), respectively, whereas the twofold features E_1 and E_2 are attributed to electronic transitions from F 1s to F 2p states covalently hybridized with Ti 4sp characters, as in the case of O K-edge XANES in TiO_2.[9,17] The detailed structure evolutions of Ti $L_{3,2}$-edge and O K-edge XANES along with phase transformation are included in the Supporting Information.

To track the local effect induced by the F ligand and to further confirm the presence of Ti^{3+}, the Ti 2p RXES spectra of APNT and NT450 are measured to reveal the Ti contribution to the valence band.[28,29,36] RXES was performed by tracking the X-ray emission (with a monochromator) resulting from the excitation of the system with photon energy tuned across the Ti $L_{3,2}$-edge. By subtracting the emission energy (Figure S3) from the corresponding excitation energies (indicated by arrows at the top of Figure 4), a series of RXES spectra are obtained in terms of energy transfer (loss) for APNT and NT450 as shown in Figure 4. Four types of spectral features are noted in the RXES spectra (bottom of Figure 4): (i) Ti 3d → Ti 2p fluorescence peak marked with purple solid bars, (ii) three charge transfer excitations (α, β, γ) from O 2p to Ti 3d states with constant energy losses,[28,29] (iii) elastic peaks with zero energy loss set as 0 eV, and (iv) a constant energy loss feature δ at ∼1.6 eV.

The overlap of the first two types of spectral features in RXES spectra 1−3 (Figure 4) and their separation in the RXES spectra 4−6 demonstrates that the dispersive emission in energy loss (purple solid bars) is fluorescence since it shows a linear relationship with the excitation energy, i.e., that the fluorescence peak moves to the high energy loss region by the same amount as the excitation energy increases, suggesting their constant emission energy (Figure S3). Next, the presence of the first two types is a signature of the strong hybridization between Ti and its O ligands ($3d^0$ of Ti^{4+} in TiO_2, thus O 2p and Ti 3d hybridization contributes to the Ti 3d → Ti 2p fluorescence), which is coherent with the two pre-edge features at the O K-edge XANES due to O 2p and Ti 3d hybridization (Figure 3 and Figure S2).

It is worth noting that the electronic structures of crystalline and amorphous TiO_2 are known to be qualitatively similar;[36] thus the presence of the additional feature at ∼1.6 eV of APNT indicates that the local environment of Ti has been modified by

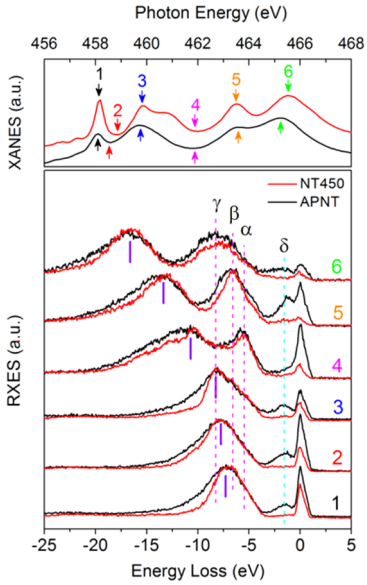

Figure 4. Ti 2p RXES spectra (bottom) of APNT (black) and NT450 (red) collected with excitation energies at the Ti $L_{3,2}$-edge TEY XANES (top panel) and plotted at an energy loss scale by subtracting the emission energy from the corresponding excitation energies, respectively.

the inclusion of the F ligand. Also, the sharp intensity reduction of the elastic scattering peaks (at 0 energy loss) upon annealing corresponds to the increase in density and hence X-ray absorption from amorphous to anatase (NT450) structures. Since RXES can be interpreted as the X-ray analogue of resonant Raman scattering and the energy transfer corresponds to an electronic excitation on the same atomic site,[27] the origin of peak δ, as its cross section increases once the excitation energies are on the resonant peaks, can be unambiguously assigned to Ti d−d interband transition due to the presence of Ti^{3+} in the TiO_2 structures;[28,29] i.e., an extra electron locates in the Ti t_{2g} orbital. Particularly, the RXES spectrum 2 also shows an intense peak δ in APNT although its excitation energy is located at the off-resonant site (the dip between t_{2g} and e_g resonances of Ti^{4+}), which further confirms the existence of rich Ti^{3+} in APNT as this excitation energy reaches the Ti^{3+} absorption resonance.[28] In addition, the energy position of the d−d transition relative to the elastic peak corresponds to the magnitude of the crystal-field splitting of $10Dq$.[29] This is illustrated in Figure 5; once the excitation energy reaches the e_g resonance, the Ti 2p core electron will be excited to the e_g states whereas the extra electron at the t_{2g} states (partially occupied) as a result of Ti^{3+} tends to fill the core hole, leading to the enhanced constant energy loss of about 1.6 eV, the energy separation between e_g and t_{2g} states; this result echoes the value of $10Dq$ obtained from Ti L_3-edge XANES.

A debate might arise here on the origin of these low energy loss features between 0 and 4 eV: the formation of Ti^{3+} in TiO_2 is derived from either intrinsic defects (e.g., oxygen vacancies) or, in this case, the self-doped F^- ions. Intrinsic defects are well-known in TiO_2, and they are responsible for the optical luminescence observed from TiO_2 nanostructures.[9,37] In particular, the broad green and strong near-infrared emissions observed in anatase and rutile TiO_2 nanostructures, respectively, are attributed to the intrinsic defects located on the surface and in the bulk.[9] However, previous Ti 2p RXES studies of both anatase[28] and rutile TiO_2[38,39] do not show any energy

DOI: 10.1021/acs.jpcc.5b11445
J. Phys. Chem. C 2016, 120, 4623−4628

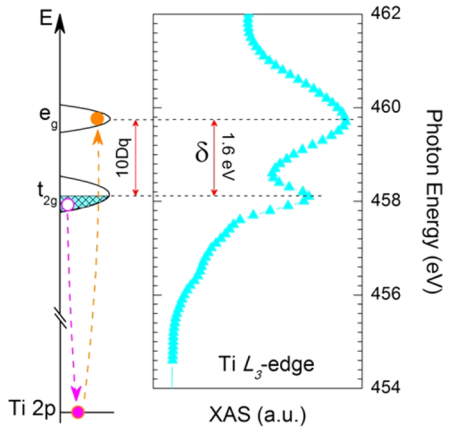

Figure 5. Schematic interpretation of d−d interband transition in terms of the magnitude of the crystal-field splitting of 10*Dq* at the Ti L_3-edge XANES of APNT. The processes denoted by dashed arrows are concerted; enegetically, it is equivalent to exciting a t_{2g} electron into the e_g via X-ray energy loss.

loss features located between 0 and 4 eV, which is in accordance with the absence of feature δ in the Ti 2p RXES of NT450 (anatase phase),[40] excluding the intrinsic defects as the cause of peak δ shown in this work.

Thus, the presence of Ti^{3+} in this study, revealed by the presence of feature δ in the Ti 2p RXES, can be unambiguously associated with the self-doped F^- ions, i.e., that the substitution of O^{2-} by F^- in the TiO_2 matrix results in the reduction of Ti^{4+} to Ti^{3+} with a d electron localized in the Ti^{3+} site. Consistently, a previous Ti 2p RXES study in the $3d^1$ system (TiF_3) by Matsubara et al.[39] showed a constant energy loss feature in both experimental and calculated results at ∼2 eV, which is quite close to our result as a pseudo-$3d^1$ system due to the self-doped F^- ions. Therefore, the strong intensity of the constant relative energy peak δ in APNT is a contribution from the surface and bulk doped F^- ions, of which the more electronegative ligand (i.e., F relative to O in this case) appears to have the effect on the localization of the electron in the t_{2g} orbital, resulting in Jahn−Teller distortion of the t_{2g} contributing to the broadening of peak δ. This result strongly shows, once and for all, that the oxygen vacancies in TiO_2, which nominally produces Ti^{3+} due to charge neutrality in the lattice, do not result in the localization of the extra electron in the Ti d orbital whereas the presence of F^- ion bonded to Ti does.

CONCLUSIONS

This work identifies and elucidates the doping centers and the chemical environment of the self-doped F^- ions and their influence on the Ti local environment of the as-grown TiO_2 NTs. Surface and bulk doping of F^- ions into the as-grown TiO_2 NTs by forming Ti−F bond is revealed by surface- and bulk-sensitive XANES, respectively, via the F K-edge. The surface doping of F^- together with the concomitant Ti^{3+}, as disclosed by XPS, can facilitate the formation of Ti−OH species on the NT surface. Consistently, RXES measured across the Ti L_3-edge XANES shows the extra Ti^{3+} band states upon F^- bulk doping, suggesting that an extra electron resides in the Ti 3d t_{2g} states by the substitution of O with F. This study establishes a benchmark in resolving the electronic effect (itinerant or localized) of incorporated dopant in electron-correlated oxide semiconductors via X-ray spectroscopic investigations.

ASSOCIATED CONTENT

Supporting Information

The Supporting Information is available free of charge on the ACS Publications website at DOI: 10.1021/acs.jpcc.5b11445.

EDX results, Ti $L_{3,2}$-edge and O K-edge XANES analysis, as well as Ti 2p RXES analysis (PDF)

AUTHOR INFORMATION

Corresponding Author

*E-mail: tsham@uwo.ca.

Notes

The authors declare no competing financial interest.

ACKNOWLEDGMENTS

Research at the University of Western Ontario is supported by the Discovery grant of the Natural Science and Engineering Research Council of Canada (NSERC), the Canada Research Chair (CRC) Program, the Canada Foundation for Innovation (CFI), and the Interdisciplinary Initiative (IDI) grant of the University of Western Ontario (UWO). The work at the Canadian Light Source (CLS) is supported by CFI, NSERC, National Research Council (NRC), Canadian Institute for Health Research (CIHR), and the University of Saskatchewan. The work at Advanced Light Source is supported by the Office of Basic Energy Sciences, of the U.S. Department of Energy under Contract No. DE-AC02-05CH11231. We would like to thank Dr. T. Regier for technical support at the SGM beamline at CLS. J.L. acknowledges the receipt of support from the CLS Graduate Student Travel Support Program. J.Z. thanks the National Natural Science Foundation of China (U1232102 and 21473178) for financial support.

REFERENCES

(1) Asahi, R.; Morikawa, T.; Ohwaki, T.; Aoki, K.; Taga, Y. Visible-Light Photocatalysis in Nitrogen-Doped Titanium Oxides. *Science* **2001**, *293*, 269−271.

(2) Gordon, T. R.; Cargnello, M.; Paik, T.; Mangolini, F.; Weber, R. T.; Fornasiero, P.; Murray, C. B. Nonaqueous Synthesis of TiO_2 Nanocrystals Using TiF_4 to Engineer Morphology, Oxygen Vacancy Concentration, and Photocatalytic Activity. *J. Am. Chem. Soc.* **2012**, *134*, 6751−6761.

(3) Chen, X. B.; Liu, L.; Yu, P. Y.; Mao, S. S. Increasing Solar Absorption for Photocatalysis with Black Hydrogenated Titanium Dioxide Nanocrystals. *Science* **2011**, *331*, 746−750.

(4) Batzill, M.; Morales, E. H.; Diebold, U. Influence of Nitrogen Doping on the Defect Formation and Surface Properties of TiO_2 Rutile and Anatase. *Phys. Rev. Lett.* **2006**, *96*, 026103.

(5) Liu, L.; Yu, P. Y.; Chen, X. B.; Mao, S. S.; Shen, D. Z. Hydrogenation and Disorder in Engineered Black TiO_2. *Phys. Rev. Lett.* **2013**, *111*, 065505.

(6) Gai, Y. Q.; Li, J. B.; Li, S. S.; Xia, J. B.; Wei, S. H. Design of Narrow-Gap TiO_2: A Passivated Codoping Approach for Enhanced Photoelectrochemical Activity. *Phys. Rev. Lett.* **2009**, *102*, 036402.

(7) Yang, H. G.; Sun, C. H.; Qiao, S. Z.; Zou, J.; Liu, G.; Smith, S. C.; Cheng, H. M.; Lu, G. Q. Anatase TiO_2 Single Crystals with A Large Percentage of Reactive Facets. *Nature* **2008**, *453*, 638−641.

(8) Ye, M. D.; Gong, J. J.; Lai, Y. K.; Lin, C. J.; Lin, Z. Q. High-Efficiency Photoelectrocatalytic Hydrogen Generation Enabled by Palladium Quantum Dots-Sensitized TiO_2 Nanotube Arrays. *J. Am. Chem. Soc.* **2012**, *134*, 15720−15723.

(9) Li, J.; Liu, L. J.; Sham, T. K. 2D XANES-XEOL Spectroscopy Studies of Morphology-Dependent Phase Transformation and Corresponding Luminescence from Hierarchical TiO_2 Nanostructures. *Chem. Mater.* **2015**, *27*, 3021−3029.

DOI: 10.1021/acs.jpcc.5b11445
J. Phys. Chem. C 2016, 120, 4623−4628

(10) Lee, S.; Park, I. J.; Kim, D. H.; Seong, W. M.; Kim, D. W.; Han, G. S.; Kim, J. Y.; Jung, H. S.; Hong, K. S. Crystallographically Preferred Oriented TiO_2 Nanotube Arrays for Efficient Photovoltaic Energy Conversion. *Energy Environ. Sci.* **2012**, *5*, 7989−7995.
(11) Regonini, D.; Bowen, C. R.; Jaroenworaluck, A.; Stevens, R. A Review of Growth Mechanism, Structure and Crystallinity of Anodized TiO_2 Nanotubes. *Mater. Sci. Eng., R* **2013**, *74*, 377−406.
(12) Gong, J. J.; Lai, Y. K.; Lin, C. J. Electrochemically Multi-Anodized TiO_2 Nanotube Arrays for Enhancing Hydrogen Generation by Photoelectrocatalytic Water Splitting. *Electrochim. Acta* **2010**, *55*, 4776−4782.
(13) Gong, J. J.; Lin, C. J.; Ye, M. D.; Lai, Y. K. Enhanced Photoelectrochemical Activities of A Nanocomposite Film with A Bamboo Leaf-Like Structured TiO_2 Layer on TiO_2 Nanotube Arrays. *Chem. Commun.* **2011**, *47*, 2598−2600.
(14) Mor, G. K.; Shankar, K.; Paulose, M.; Varghese, O. K.; Grimes, C. A. Use of Highly-Ordered TiO_2 Nanotube Arrays in Dye-Sensitized Solar Cells. *Nano Lett.* **2006**, *6*, 215−218.
(15) Macak, J. M.; Tsuchiya, H.; Ghicov, A.; Schmuki, P. Dye-Sensitized Anodic TiO_2 Nanotubes. *Electrochem. Commun.* **2005**, *7*, 1133−1137.
(16) Fang, H. T.; Liu, M.; Wang, D. W.; Sun, T.; Guan, D. S.; Li, F.; Zhou, J. G.; Sham, T. K.; Cheng, H. M. Comparison of the Rate Capability of Nanostructured Amorphous and Anatase TiO_2 for Lithium Insertion Using Anodic TiO_2 Nanotube Arrays. *Nanotechnology* **2009**, *20*, 225701.
(17) Zhou, J. G.; Fang, H. T.; Maley, J. M.; Murphy, M. W.; Ko, J. Y. P.; Cutler, J. N.; Sammynaiken, R.; Sham, T. K.; Liu, M.; Li, F. Electronic Structure of TiO_2 Nanotube Arrays from X-ray Absorption Near Edge Structure Studies. *J. Mater. Chem.* **2009**, *19*, 6804−6809.
(18) Shrestha, N. K.; Macak, J. M.; Schmidt-Stein, F.; Hahn, R.; Mierke, C. T.; Fabry, B.; Schmuki, P. Magnetically Guided Titania Nanotubes for Site-Selective Photocatalysis and Drug Release. *Angew. Chem., Int. Ed.* **2009**, *48*, 969−972.
(19) Song, Y. Y.; Schmidt-Stein, F.; Bauer, S.; Schmuki, P. Amphiphilic TiO_2 Nanotube Arrays: An Actively Controllable Drug Delivery System. *J. Am. Chem. Soc.* **2009**, *131*, 4230−4232.
(20) Mun, K. S.; Alvarez, S. D.; Choi, W. Y.; Sailor, M. J. A Stable, Label-Free Optical Interferometric Biosensor Based on TiO_2 Nanotube Arrays. *ACS Nano* **2010**, *4*, 2070−2076.
(21) Alivov, Y.; Fan, Z. Y. A TiO_2 Nanostructure Transformation: from Ordered Nanotubes to Nanoparticles. *Nanotechnology* **2009**, *20*, 405610.
(22) Tosoni, S.; Fernandez Hevia, D.; Gonzalez Diaz, O.; Illas, F. Origin of Optical Excitations in Fluorine-Doped Titania from Response Function Theory: Relevance to Photocatalysis. *J. Phys. Chem. Lett.* **2012**, *3*, 2269−2274.
(23) Yu, J. C.; Yu, J. G.; Ho, W. K.; Jiang, Z. T.; Zhang, L. Z. Effects of F-Doping on the Photocatalytic Activity and Microstructures of Nanocrystalline TiO_2 Powders. *Chem. Mater.* **2002**, *14*, 3808−3816.
(24) Xiong, H.; Slater, M. D.; Balasubramanian, M.; Johnson, C. S.; Rajh, T. Amorphous TiO_2 Nanotube Anode for Rechargeable Sodium Ion Batteries. *J. Phys. Chem. Lett.* **2011**, *2*, 2560−2565.
(25) Naduvath, J.; Bhargava, P.; Mallick, S. Mechanism of Formation of Faceted Titania Nanoparticles from Anodized Titania Nanotubes. *J. Phys. Chem. C* **2015**, *119*, 9574−9579.
(26) Czoska, A. M.; Livraghi, S.; Chiesa, M.; Giamello, E.; Agnoli, S.; Granozzi, G.; Finazzi, E.; Di Valentin, C.; Pacchioni, G. The Nature of Defects in Fluorine-Doped TiO_2. *J. Phys. Chem. C* **2008**, *112*, 8951−8956.
(27) Parks Cheney, C.; Vilmercati, P.; Martin, E. W.; Chiodi, M.; Gavioli, L.; Regmi, M.; Eres, G.; Callcott, T. A.; Weitering, H. H.; Mannella, N. Origins of Electronic Band Gap Reduction in Cr/N Codoped TiO_2. *Phys. Rev. Lett.* **2014**, *112*, 036404.
(28) Augustsson, A.; Henningsson, A.; Butorin, S. M.; Siegbahn, H.; Nordgren, J.; Guo, J. H. Lithium Ion Insertion in Nanoporous Anatase TiO_2 Studied with RIXS. *J. Chem. Phys.* **2003**, *119*, 3983−3987.
(29) Higuchi, T.; Tsukamoto, T.; Watanabe, M.; Grush, M. M.; Callcott, T. A.; Perera, R. C.; Ederer, D. L.; Tokura, Y.; Harada, Y.; Tezuka, Y.; et al. Crystal-Field Splitting and the On-Site Coulomb Energy of $La_xSr_{1-x}TiO_3$ from Resonant Soft-X-ray Emission Spectroscopy. *Phys. Rev. B: Condens. Matter Mater. Phys.* **1999**, *60*, 7711−7714.
(30) Regier, T.; Paulsen, J.; Wright, G.; Coulthard, I.; Tan, K.; Sham, T. K.; Blyth, R. I. R. Commissioning of the Spherical Grating Monochromator Soft X-ray Spectroscopy Beamline at the Canadian Light Source. *AIP Conf. Proc.* **2006**, *879*, 473−476.
(31) Li, J.; Sham, T. K.; Ye, Y.; Zhu, J.; Guo, J. Structural and Optical Interplay of Palladium-Modified TiO_2 Nanoheterostructure. *J. Phys. Chem. C* **2015**, *119*, 2222−2230.
(32) Yang, H. M.; Zhang, X. C. Synthesis, Characterization and Computational Simulation of Visible-Light Irradiated Fluorine-Doped Titanium Oxide Thin Films. *J. Mater. Chem.* **2009**, *19*, 6907−6914.
(33) Li, Z. D.; Wang, F.; Kvit, A.; Wang, X. D. Nitrogen Doped 3D Titanium Dioxide Nanorods Architecture with Significantly Enhanced Visible Light Photoactivity. *J. Phys. Chem. C* **2015**, *119*, 4397−4405.
(34) Fang, W. Q.; Wang, X. L.; Zhang, H. M.; Jia, Y.; Huo, Z. Y.; Li, Z.; Zhao, H. J.; Yang, H. G.; Yao, X. D. Manipulating Solar Absorption and Electron Transport Properties of Rutile TiO_2 Photocatalysts via Highly n-Type F-Doping. *J. Mater. Chem. A* **2014**, *2*, 3513−3520.
(35) Gao, Y. F.; Masuda, Y.; Peng, Z. F.; Yonezawa, T.; Koumoto, K. Room Temperature Deposition of A TiO_2 Thin Film from Aqueous Peroxotitanate Solution. *J. Mater. Chem.* **2003**, *13*, 608−613.
(36) Stromme, M.; Ahuja, R.; Niklasson, G. A. New Probe of the Electronic Structure of Amorphous Materials. *Phys. Rev. Lett.* **2004**, *93*, 206403.
(37) Knorr, F. J.; Zhang, D.; McHale, J. L. Influence of $TiCl_4$ Treatment on Surface Defect Photoluminescence in Pure and Mixed-Phase Nanocrystalline TiO_2. *Langmuir* **2007**, *23*, 8686−8690.
(38) Harada, Y.; Kinugasa, T.; Eguchi, R.; Matsubara, M.; Kotani, A.; Watanabe, M.; Yagishita, A.; Shin, S. Polarization Dependence of Soft-X-ray Raman Scattering at the L Edge of TiO_2. *Phys. Rev. B: Condens. Matter Mater. Phys.* **2000**, *61*, 12854−12859.
(39) Matsubara, M.; Uozumi, T.; Kotani, A.; Harada, Y.; Shin, S. Polarization Dependence of Resonant X-ray Emission Spectra in Early Transition Metal Compounds. *J. Phys. Soc. Jpn.* **2000**, *69*, 1558−1565.
(40) Chen, C. L.; Dong, C. L.; Chen, C. H.; Wu, J. W.; Lu, Y. R.; Lin, C. J.; Liou, S. Y. H.; Tseng, C. M.; Kumar, K.; Wei, D. H.; et al. Electronic Properties of Free-Standing TiO_2 Nanotube Arrays Fabricated by Electrochemical Anodization. *Phys. Chem. Chem. Phys.* **2015**, *17*, 22064−22071.

DOI: 10.1021/acs.jpcc.5b11445
J. Phys. Chem. C 2016, 120, 4623−4628